

Cite this: *J. Mater. Chem. A*, 2013, **1**, 2533

## Rigid bio-foam plastics with intrinsic flame retardancy derived from soybean oilt

Jun Feng Qiu,<sup>ab</sup> Ming Qiu Zhang,<sup>b</sup> Min Zhi Rong,<sup>\*b</sup> Su Ping Wu<sup>ab</sup> and József Karger-Kocsis<sup>c</sup>

Acrylated epoxidized soybean oil was chemically grafted with difunctional flame retardants carrying phosphorus, double bonds or biphenyl groups, and then copolymerized with styrene to produce bio-foams with high mechanical properties and intrinsic flame resistance. Owing to the introduction of rigid comonomer, phosphorus, additional double bonds or biphenyl side groups, the bio-foams showed compressive strength similar to that of conventional unsaturated polyester foam, antiflaming capability and biodegradability as well. More importantly, the modified flame retardant partially took the role of styrene, leading to a lower fraction of petroleum based substance in the bio-foams without the expense of foam strength, and improved biodegradability. The comparison between the bio-foams with intrinsic flame retardancy on a molecular level and those containing inflaming retardant fillers revealed that the latter have acquired rather poor mechanical properties and hence are obviously inferior to the former in practical applications where a load-bearing capability is required.

Received 25th October 2012

Accepted 12th December 2012

DOI: 10.1039/c2ta01404a

[www.rsc.org/MaterialsA](http://www.rsc.org/MaterialsA)

## Introduction

There is a growing urgency to develop bio-based products and other innovative technologies that can relieve the widespread dependence on fossil fuels.<sup>1-3</sup> A qualifying bio-based product derived from renewable resources should possess attractive properties like recycling capability, triggered biodegradability (*i.e.*, stable in their intended lifetime, but biodegrade after disposal in composting conditions), commercial viability and environmental acceptability.

When looking at packaging materials used in our daily life, we find that they are mostly non-biodegradable foam plastics and the discarded packaging increases burden on the environment. Therefore, it would be very appealing to manufacture their substitutes based on bio-resources. Compared to biodegradable bulk plastics, which have become competitive in the markets dominated by the products based on petroleum feedstock, bio-foams developed so far still require more work for practical application. For example, a few researchers have

started to prepare starch-based foams<sup>4-15</sup> and natural fiber/starch foam composites,<sup>16-18</sup> but there are long stretches to reach their target usages in fast food packaging and containers owing to their poor overall properties and high cost.

In recent years, plant oils have attracted increasing attention as non-petroleum raw materials. Polyurethane (PU) foam plastics using vegetable oil derivatives as polyols were prepared. Semi-rigid PU foams, for example, were made of castor oil carrying hydroxyl groups.<sup>19-21</sup> In addition, rigid PU foams were also produced by using modified soy-based polyols.<sup>22,23</sup> In our efforts to synthesis bio-foam plastics with plant oil triglycerides, radical polymerization of maleic anhydride modified castor oil (MACO) and acrylated epoxidized soybean oil (AESO) was adopted.<sup>24-28</sup> It was proven that the mechanical performance and biodegradability of the resulting materials can be easily tailored *via* adjusting the feeding ratio of vinyl-functionalized plant oils to diluent monomers. Moreover, these bio-foam plastics show better biodegradability than those plant oils derived PU foams.<sup>24</sup>

However, it is worth noting that all the plant oils based bio-foams exhibit lower compressive strength and modulus in comparison with conventional unsaturated polyester (UP) foams from fossil oil,<sup>24,25</sup> which limits their applications where a load-bearing capacity is required. In addition, flame retardancy, a basic requirement for foamed materials, has not yet been studied in the area of bio-foam plastics. It is an obvious challenge to simultaneously provide bio-foams with high rigidity and flame resistance. As a class of flame retardants, appropriate intumescence flame retardants can be incorporated to interrupt the self-sustained combustion of a polymer at its earliest stage.

<sup>a</sup>Key Laboratory for Polymeric Composite and Functional Materials of Ministry of Education, DSAPM Lab, School of Chemistry and Chemical Engineering, Sun Yat-sen (Zhongshan) University, Guangzhou, 510275, P. R. China

<sup>b</sup>Materials Science Institute, Sun Yat-sen (Zhongshan) University, Guangzhou 510275, P. R. China. E-mail: cesrmz@mail.sysu.edu.cn; Fax: +86-020-84114008; Tel: +86-20-84114008

<sup>c</sup>Department of Polymer Engineering, Budapest University of Technology and Economics, H-1111 Budapest, Hungary

† Electronic supplementary information (ESI) available: Change of acid number with reaction time during FRC-6-MA synthesis. Thermal stability of AESO/St, FR-AESO/St and DOPOMA-AESO/St foams. See DOI: 10.1039/c2ta01404a



The protection mechanism lies in the fact that the charred layer serves as a physical barrier, which slows down heat and mass transfer between the gas and condensed phases. However, the intumescent systems have to be less efficient in foam materials characterized by a cellular structure filled with abundant air. If a large amount of flame retardant is added to keep high level flame resistance, the mechanical properties of the foams must be greatly deteriorated. In this context, the synthesis of intrinsically antiflaming bio-foams might be a possible solution.

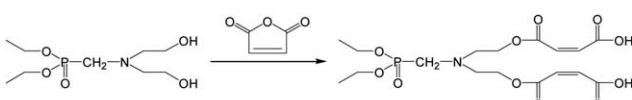
To prepare a bio-resin suited for sheet molding compound (SMC) applications, Wool and his co-workers further modified AESO by adding maleic anhydride, which renders the molecules acid groups and more unsaturation.<sup>29,30</sup> Inspired by their work, we choose two kinds of phosphorus-containing flame retardant as starting agents, which firstly react with maleic anhydride to form new reactive modifiers (Schemes 1 and 2), and then they are applied to react with AESO. Afterwards, the resultant monomers are copolymerized with different amounts of styrene to create rigid foam plastics. As a result, the foams are integrated with, not only phosphorus, but also additional double bonds or biphenyl groups. The former would account for the flame retarding ability, while the latter induces higher cross-linking density or molecular rigidity and hence higher mechanical strength.

In the present paper, synthetic conditions, chemical structure, mechanical properties, flame retardancy and biodegradability of the products are studied in detail to reveal the effects of the aforesaid difunctional modifiers. It is hoped that novel intrinsically antiflaming bio-forms can thus be obtained from soybean oil, which possess mechanical properties comparable to conventional petro-based unsaturated polyester foams, satisfied biodegradability and evident flame retardancy.

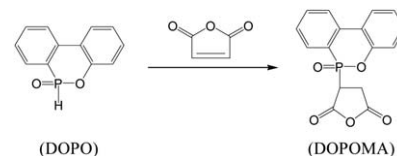
## Experimental

### Materials

ESO (industrial product) with 3.9 epoxide groups per triglyceride was purchased from Xin Jin Long Plastics Ltd. Co., China. Both acrylic acid (C.P.) and maleic anhydride (MA, C.P.) were supplied by Tianjin Damao Chemical Factory, China. The comonomer, styrene (St, C.P.) was supplied by Tianjin Fuchen Chemical Factory, China. The curing initiator, benzoyl peroxide (BPO, A.R.) was produced by Guangzhou Chemical Reagent Co., China. The curing accelerant, *N,N*-dimethyl aniline, was supplied by Shantou Guanghua Chemical Co., China. NaHCO<sub>3</sub> (A.R.) produced by Guangzhou Chemical Co., China was used as the blowing agent. The surfactant, Tween 80 (polyoxyethylene sorbitan monooleate, C.P.) was purchased from Tianjin Medicine Co., China. The flame retardants, diethyl bis(2-hydroxyethyl) amino methyl



**Scheme 1** Schematic illustration of the reaction of flame retardant FRC-6 with maleic anhydride to produce FRC-6-MA.



**Scheme 2** Schematic illustration of the reaction of flame retardant DOPO with maleic anhydride to produce DOPOMA.

phosphonate (trade name: FRC-6) and 9,10-dihydro-9-oxa-10-phosphaphenanthrene-10-oxide (DOPO) were provided by Zhejiang Wansheng Chemical Co., China and Jiangsu Huihong Jinpu Chemical Co., China, respectively. Other reagents and solvents were conventionally available commercial products. All the chemicals were used without further purification. Acrylated epoxidized soybean oil (AESO), which has an average of 2.9 acrylates per triglyceride, was prepared according to ref. 25.

### Synthesis of maleated flame retardants

The two hydroxyl groups on the flame retardant FRC-6 molecule react with maleic anhydride to form the reactive modifier FRC-6-MA as follows (Scheme 1). Maleic anhydride (MA, 39.2 g) and FRC-6 liquid (51 g) (2 : 1 by mole) were added into a 250 ml four-necked round bottom flask equipped with a stirrer, a thermometer and an inlet of dry nitrogen. The reaction proceeded with continuous stirring at 90 °C for a period of time (1–2 h) without any solvent or catalyst. Meanwhile, the acid numbers at different reaction times were determined to monitor the reaction procedure. When the acid number attained 250 mg KOH per g, the reaction stopped, and the product FRC-6-MA was directly used as the modifier.

Similarly, flame retardant DOPO can react with maleic anhydride at the mole ratio of 1 : 1 (Scheme 2). Typically, 1 mol DOPO (216 g) and 300 g xylene were charged into a 1000 ml four-necked round-bottom flask equipped with a stirrer, a thermometer, and an inlet of dry nitrogen. When the solution was heated to 80 °C, 1 mol (98 g) maleic anhydride in 300 g THF solution was added dropwise within 2 h while keeping the solution temperature constant. The reaction was completed for additional 24 h at 80 °C under N<sub>2</sub> atmosphere and then cooled down to room temperature. Afterwards, the white powder product DOPOMA was collected by removal of solvent using rotary evaporator, washing and drying.

### Synthesis of FRC-6-MA and DOPOMA grafted AESO

FRC-6-MA and AESO (mole ratio = 0.5 : 1–3 : 1) were added in a 500 ml four-necked round bottom flask equipped with a stirrer, a thermometer and an inlet of dry nitrogen. Typically, when the mole ratio was 1 : 1, 35.3 g FRC-6-MA and 122.2 g AESO were used. Equal weight toluene as the solvent was then added with 0.1% hydroquinone acting as the inhibitor and 1% sulphuric acid or *p*-toluene sulfonic acid as the catalyst. The reaction proceeded with continuous stirring at reflux temperatures for 6–8 h. Meanwhile, the acid numbers at different reaction times were determined to monitor the course of the reaction. When

the system did not show an obvious change in acid value and generate water in the segregator, the reaction was stopped. Then, the product of FRC-6-MA grafted AESO (FR-AESO) was collected by the removal of solvent using a rotary evaporator.

To synthesize different DOPOMA grafted AESO monomers (DOPOMA-AESO), the necessary amount of DOPOMA and AESO (mole ratio = 0.5 : 1–1.5 : 1) was added into a 500 ml four-necked round bottom flask equipped with a stirrer, a thermometer and an inlet of dry nitrogen. Typically, when the mole ratio was 0.42 : 1, 26.4 g DOPOMA and 244.4 g AESO were used. The mixture was then heated up to 100 °C and DOPOMA began to dissolve and react with AESO without catalyst. When the reaction proceeded for 2–3 h until all the white powder of DOPOMA disappeared, the reaction stopped and the product was directly used as the monomer.

### Preparation of bio-foam plastics from AESO, FR-AESO and DOPOMA-AESO monomers

The synthesized AESO, FR-AESO or DOPOMA-AESO was firstly mixed with comonomer St (80 : 20, 70 : 30, 60 : 40 by weight), initiator (BPO, 4 phr, *i.e.*, 4 parts per hundred parts of base resin by weight), accelerants (*N,N*-dimethyl aniline, 0.4 phr), surfactant (Tween 80, 2 phr), and blowing agent (NaHCO<sub>3</sub>, different amounts according to the required foam density) in a cup. After agitation at 74 °C for several minutes when the mixture became viscous, a little water (4 phr) was added into the system, and then the mixture was quickly stirred until it became white and was poured into a special open mold to foam and set. Post-curing at 100 °C for 2 h was applied. For AESO foams, both NaHCO<sub>3</sub> (1.5 phr) and acrylic acid (3.6 phr) were used as blowing agents, while other foams only used NaHCO<sub>3</sub> (1.5 phr), because carboxyl groups existed on the molecules of FR-AESO and DOPOMA-AESO.

The FR-AESO/St foams made from FR-AESO with molar ratio of FRC-6-MA/AESO = 1 : 1, and the DOPOMA-AESO/St foams from DOPOMA-AESO with molar ratio of DOPOMA/AESO = 0.5 : 1, were subjected to mechanical, pyrolytic and biodegradation tests.

For comparison of the mechanical properties, a commercial product of unsaturated polyester (UP, 191C) was used to prepare the plastic foams. The foaming procedure was identical to that applied for making AESO foams, except that the ratio of UP/St was set at 70/30.

In order to elucidate the shortcomings of extrinsic inflaming retardancy, an intumescent flame retardant (IFR, Guangzhou Xin Mei Chemical Co., China) including three ingredients (*i.e.* an acid source (ammonium polyphosphate, APP), a char forming agent (pentaerythritol, PER) and a blowing agent (melamine, M) at the ratio of APP/PER/M = 3/1/1) was added into the AESO monomer mixtures, and then the foams (IFR-AESO/St) with different contents of IFR were prepared by the same foaming procedure.

### Characterization

The acid number was measured according to the procedure described in ref. 24. The molecular structures of FR-AESO and

DOPOMA-AESO were analyzed by <sup>1</sup>H-nuclear magnetic resonance (NMR, VARIAN Mercury-Plus 300) and Fourier transform infrared (FTIR, BRUKER EQUINOX 55) spectrometers, respectively.

Apparent density of the foams (*i.e.* the weight of foam per unit volume) was measured according to an ASTM D 1622-03 standard. Compressive properties of the foams were evaluated by a LWK-5 universal tester (Guangzhou Instrument Co. Ltd., China) following the procedure specified in ASTM D 1621-00 or ISO 844 standard. The specimen was a column with diameter of 42.5 mm and height of 36 mm, which was compressed between two stainless steel plates at a crosshead speed of 10 mm min<sup>-1</sup>. The compression force was applied in parallel to the foam rise direction. To eliminate the influence of foam density on the compressive properties, the compressive stress was normalized by the sample density. As a result, a specific stress (*i.e.* stress/density with the unit of m), rather than stress was used on the stress-strain curves. The razor-cut surfaces, as well as the fractured surfaces, by tearing were investigated by a Hitachi S-520 scanning electron microscope (SEM). Prior to the observation, all the samples were gold coated.

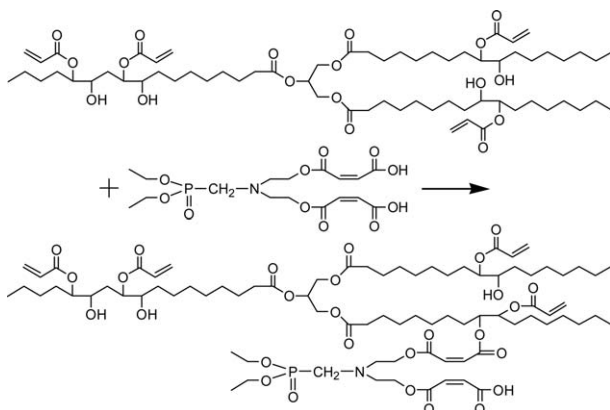
Thermogravimetric analysis (TGA) was performed on a Netzsch TG209 thermogravimetric analyzer at a heating rate of 20 °C min<sup>-1</sup> under nitrogen. Limiting oxygen index (LOI) was measured by a Stanton Redcroft flame meter based on the Chinese standard GB/T 2406-2009. The critical percentage O<sub>2</sub> in the O<sub>2</sub>-N<sub>2</sub> mixture that supported combustion of the sample was taken as LOI. Vertical burning tests were conducted on FTT UL 94 horizontal/vertical flame chamber following ANSI/UL-94-1985 VF (Vertical Foam) standard (sample size: 127 × 12.7 × 12.7 mm<sup>3</sup>).

The degree and rate of aerobic biodegradation of the AESO foams were determined in terms of soil burial under laboratory conditions. The foams were cut into slices with thickness of about 4 mm, and then buried in soil. The soil in a beaker was kept in an oven controlled at the desired temperature (30 °C). The soil composition and compost conditions resembled those described in ASTM D 5988-03. After a given time, the samples were taken out of the container, washed thoroughly and dried in vacuum. Variations in weight and cells morphology before and after the biodegradation were evaluated. The change in cellular structure of the foams was observed by SEM.

## Results and discussion

### Synthesis and characterization of FR-AESO and DOPOMA-AESO monomers

Since the flame retardant FRC-6 has two hydroxyl groups, two moles of maleic anhydride were used to stoichiometrically react with one mole of FRC-6 to form FRC-6-MA. As the reaction proceeds, the acid number drastically decreases at the beginning, and then levels off due to the reduction of the component's concentration (Fig. S1†). Finally, an acid number of 250 mg KOH per g was achieved after 2 h, which is very close to the theoretical value of 248.8 mg KOH per g, indicating that FRC-6-MA has been obtained as expected. The subsequent graft reaction of FRC-6-MA with hydroxyl groups of AESO (Scheme 3)



**Scheme 3** Schematic illustration of the reaction between FRC-6-MA and AESO to produce FR-AESO.

belongs to esterification, which is auto-catalyzed by the carboxyl groups of FRC-6-MA. Because reactivity of the secondary hydroxyl on AESO is quite low, however, the auto-catalytic effect is not strong enough to accelerate the reaction (Fig. 1). Therefore, additional catalyst of 1 wt% sulphuric acid ( $H_2SO_4$ ) or *p*-toluene sulfonic acid (P-TSA) is used, leading to a much faster reaction and lower acid numbers than the control system. Comparatively, sulphuric acid shows higher catalysis efficiency owing to its great acidity that favors the nucleophilic addition reaction of hydroxyl groups.

FTIR spectra of FR-AESO and AESO are given in Fig. 2. In comparison with the spectrum of AESO, the peak at  $3469\text{ cm}^{-1}$  ascribing to  $-\text{OH}$  absorption is evidently decreased on the spectrum of FR-AESO, while the peaks at  $1635\text{ cm}^{-1}$  of  $-\text{C}=\text{C}-$  double bond and  $1740\text{ cm}^{-1}$  of carbonyl groups are enhanced. No peaks corresponding to cyclic anhydride at  $1790$  and  $1850\text{ cm}^{-1}$  can be perceived in the resultant FR-AESO,<sup>31</sup> meaning that almost all the maleic anhydride has been consumed during the preparation of FRC-6-MA. Fig. 3(a) illustrates that most peaks of FR-AESO on the  $^1\text{H-NMR}$  spectrum are similar to those of AESO, except that two new peaks emerge at  $6.90\text{ ppm}$  (8) and  $6.22\text{ ppm}$  (7) as shown in Fig. 3(b), which correspond to the absorptions of

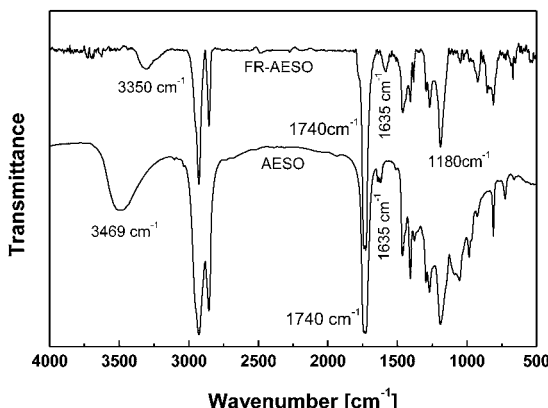


**Fig. 2** FTIR spectra of AESO and FR-AESO.

FRC-6 ( $\text{P}-\text{CH}_2-\text{N}$ ) protons and double bonds protons of maleate, respectively. Moreover, the peak ascribing to the protons of original maleic anhydride at  $7.03\text{ ppm}$  is no longer detected. Since the peaks in the range  $5.8\text{--}6.6\text{ ppm}$  representing the two protons of maleate overlap that of the acrylate group, the content of FR-AESO per triglyceride,  $N_{\text{maleate}}$ , can be quantitatively determined by deducting the acrylate moles from the total double bonds moles:

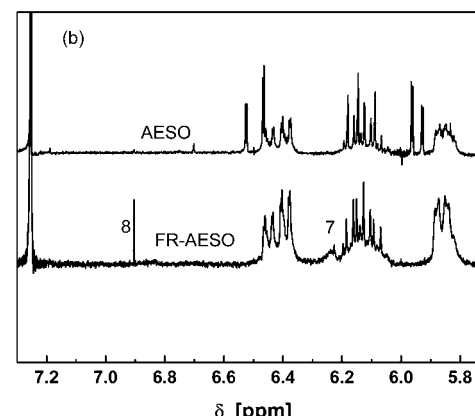
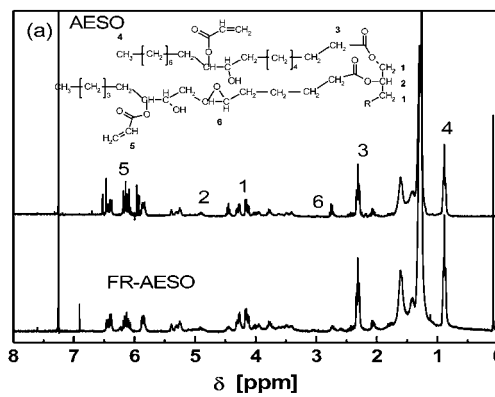


**Fig. 3**  $^1\text{H-NMR}$  spectra of AESO and FR-AESO ( $n(\text{FRC-6-MA}) : n(\text{AESO}) = 1 : 1$ ; catalyst: 1 wt%  $H_2SO_4$ ,  $120\text{ }^\circ\text{C}$ , 8 h) with peak assignments.

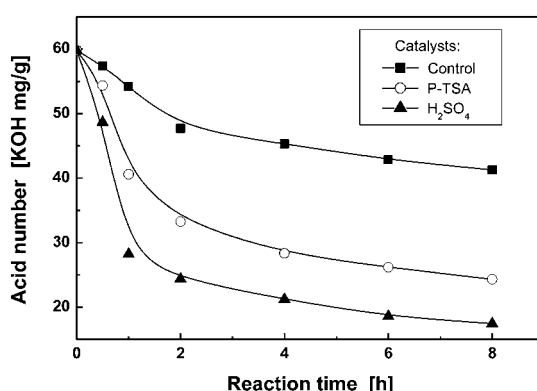


**Fig. 1** Dependence of acid number on reaction time during FR-AESO synthesis with different catalysts (molar ratio of FRC-6-MA to AESO = 1 : 1; P-TSA: *p*-toluene sulfonic acid).

$$N_{\text{maleate}} = \frac{1}{2} \left( \frac{A_{5.8-6.6 \text{ ppm}}}{A_{\text{proton}}} - 2.87 \times 3 \right) \quad (1)$$

where  $A_{5.8-6.6 \text{ ppm}}$  denotes the peak integral of all  $\text{C}=\text{C}$  groups appearing at 5.8–6.6 ppm, and the single proton peak area resulting from the methyl protons peak at 0.9 ppm ( $-\text{CH}_3$ ) of fatty acids, which acts as the internal standard. When 2.87 mol acrylates per triglyceride that possess three protons in AESO molecule is taken off, it is known that 1.25 moles of FRC-6-MA are attached to one triglyceride molecule for the system with a mole feeding ratio of FRC-6-MA : AESO = 1 : 1. Since each FRC-6-MA has two double bonds, 5.37 active double bonds per triglyceride are estimated to be included in FR-AESO.

The P–H group in DOPO is reactive towards some groups such as vinyl, oxirane and carbonyl.<sup>32</sup> Accordingly, an addition reaction between DOPO and maleic anhydride equivalently performs, producing DOPOMA. The  $^1\text{H-NMR}$  spectra in Fig. 4 confirms the products of the reaction between  $-\text{P}(\text{O})-\text{H}$  groups of DOPO and  $\text{C}=\text{C}$  groups of maleic anhydride. On the spectrum of DOPOMA, the peak related with P–H of DOPO at 9.0 ppm (9) disappears, while two new peaks coming from MA protons appear at 3.5 ppm (9) and 2.7 ppm (10), which represent the P atom connected to the cyclic carbon atom of maleic anhydride. Moreover, other peaks in the range of 7–8 ppm belonging to the protons of biphenyl groups of DOPOMA resemble those of DOPO, but shift to lower-field due to the

electron-withdrawing effect of the attached maleic anhydrite groups.

With the further reaction of DOPOMA with AESO *via* esterification, a DOPOMA-substituted AESO (DOPOMA-AESO) is yielded (Scheme 4). Evidently, it is a simple and convenient way to generate a plant oil based resin containing phosphorous compound. Fig. 5 compares the  $^1\text{H-NMR}$  spectrum of DOPOMA-AESO with that of AESO. We can see that several new peaks are observed at 7–8 ppm, which originate from the biphenyl protons of DOPO. The result demonstrates that the envisaged reaction between AESO and DOPOMA has occurred. Similarly, by taking the peaks at 0.9 ppm ( $-\text{CH}_3$ ) as a reference, it is calculated from the integral of the peaks at 7–8 ppm that 0.42 mol DOPOMA is attached to AESO. That is, about 15% hydroxyl groups of AESO have taken part in the reaction. Other peaks of DOPOMA-AESO have similar profiles and positions as AESO, indicating that the reaction follows an identical process without side reactions.

### Mechanical properties and flame retardancy of AESO, FR-AESO and DOPOMA-AESO foams

The specific stress–strain curves of FR-AESO/St foams are shown in Fig. 6, which are similar to the behavior of elastomer-like AESO/St foams.<sup>25</sup> However, a careful survey of the deformation

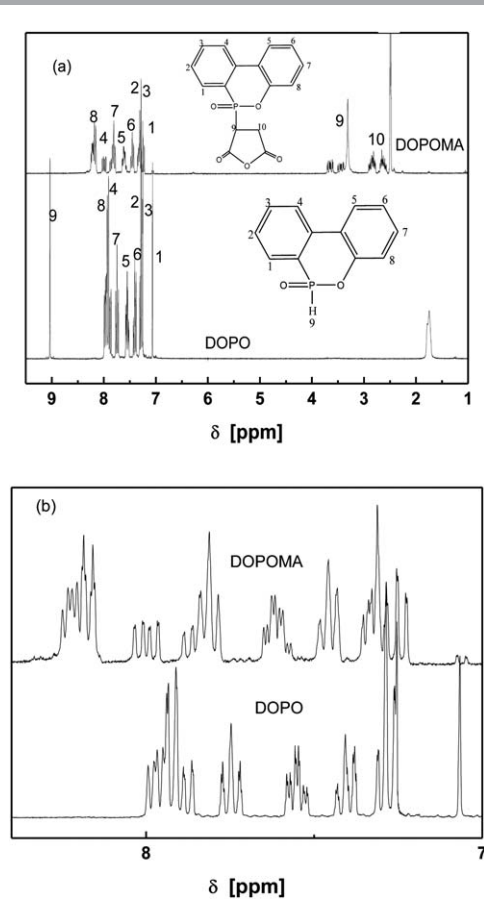
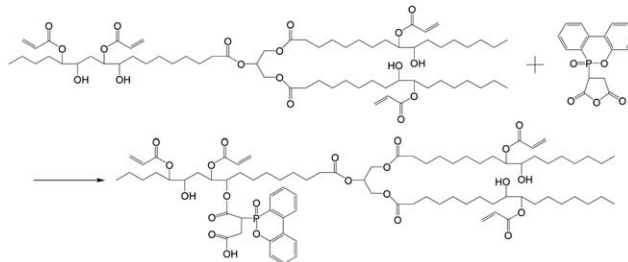


Fig. 4  $^1\text{H-NMR}$  spectra of DOPO and DOPOMA with peak assignments.



Scheme 4 Schematic illustration of the reaction between DOPOMA and AESO to produce DOPOMA-AESO.

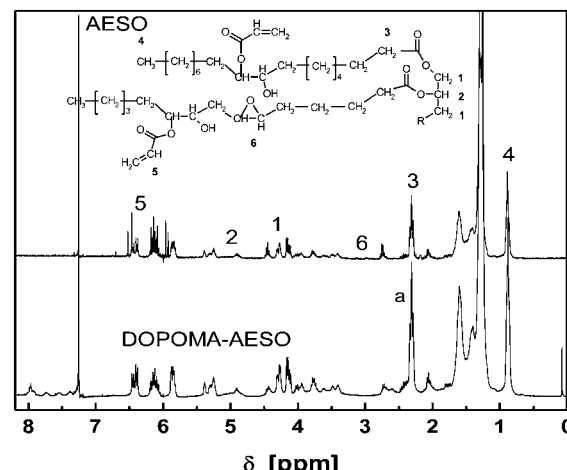
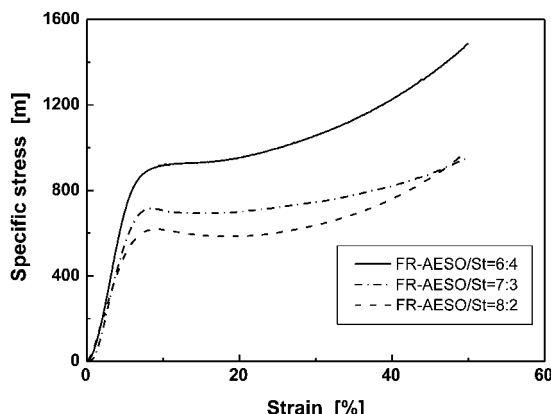


Fig. 5  $^1\text{H-NMR}$  spectra with peak assignments of AESO and DOPOMA-AESO ( $n(\text{DOPOMA}) : n(\text{AESO}) = 0.42 : 1$ ).



**Fig. 6** Typical compressive specific stress–strain curves of FR-AESO/St foams with different styrene contents (density:  $0.220 \pm 0.005 \text{ g cm}^{-3}$ ).

feature reveals that all the FR-AESO/St foams exhibit yielding when the content of St is over 20 wt%, while AESO/St foams could not yield when St content is less than 30 wt%. This phenomenon reflects that FR-AESO/St foams are more rigid than AESO/St foams. FR-AESO contains more reactive double bonds than AESO, leading to a higher crosslink density that is responsible for the foam rigidity. As a result, the relative increases in specific compressive stress and the modulus of FR-AESO/St (80/20) foam in comparison to AESO/St (80/20) foam are 63 and 36%, respectively. It manifests that the molecular level modification of AESO with flame retardant FRC-6-MA results in a considerable enhancement of mechanical properties.

Moreover, although both the specific compressive strength and modulus of the foams increase with the content of styrene (Fig. 7), the compressive modulus of FR-AESO/St foams at higher St content gradually approaches that of AESO/St foams (Fig. 7(b)). This implies that polystyrene plays a leading role in the stiffening of the foams. As for DOPOMA-AESO/St foams, they have a similar compressive strength and modulus as FR-AESO/St (Fig. 7), but much lower failure strain (Fig. 8). Evidently, the biphenyl side groups of DOPOMA make the critical contribution. On the whole, the above results reveal that an increase of double bonds, integration of rigid comonomer and attachment of rigid side groups can bring about different reinforcement effects of the foams of plant oils.

To further elucidate the feasibility of FR-AESO/St and DOPOMA-AESO/St foams employed as structural materials, the compressive behaviors of the flame retarding bio-foams are compared with that of the foam made from traditional unsaturated polyester (UP) in Fig. 9. It is seen that UP foam is a typical brittle material, while the bio-foams are stronger and tougher materials. The distinct mechanical responses can be understood from the angle of molecular structures of the materials. In general, thermosetting unsaturated polyester resin consists of phthalic anhydride, maleic anhydride and ethylene glycol, in which aromatic reactant is added to improve hardness, rigidity and heat resistance of the crosslinked product. AESO only contains aliphatic components and hence is endowed with

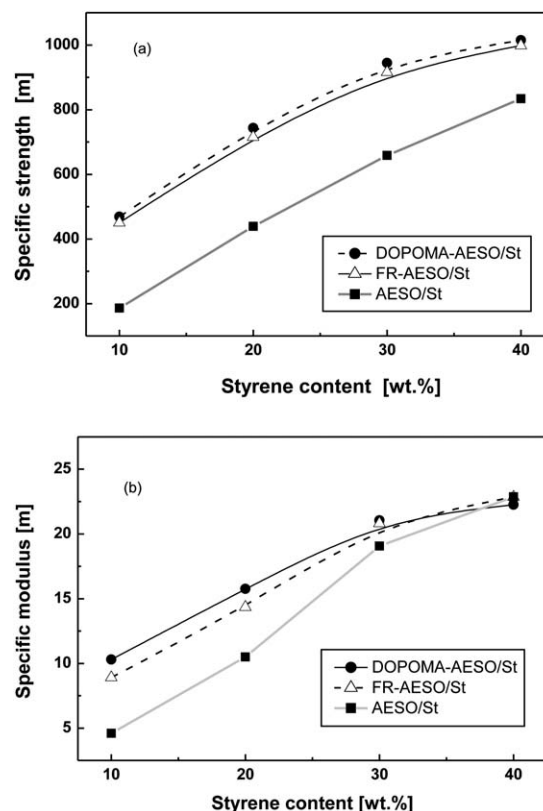


**Fig. 7** (a) Specific compressive strength and (b) modulus of AESO/St, FR-AESO/St and DOPOMA-AESO/St foams as a function of styrene content (density:  $0.220 \pm 0.005 \text{ g cm}^{-3}$ ).

remarkable flexibility. At least 50 wt% styrene was needed for AESO/St foam to have a similar compressive strength as UP/St (70/30) foam.<sup>25</sup> Nevertheless, because FR-AESO possesses quite a lot of double bonds (about 5.4 per molecule) and biphenyl groups are attached to DOPOMA-AESO, both the bio-foams have acquired comparable or even higher compressive strengths with reference to the data of UP/St foam (Fig. 9), despite the former containing an obviously lower content of styrene (20 wt%) than the latter (30 wt%). Under the circumstances, it is known that

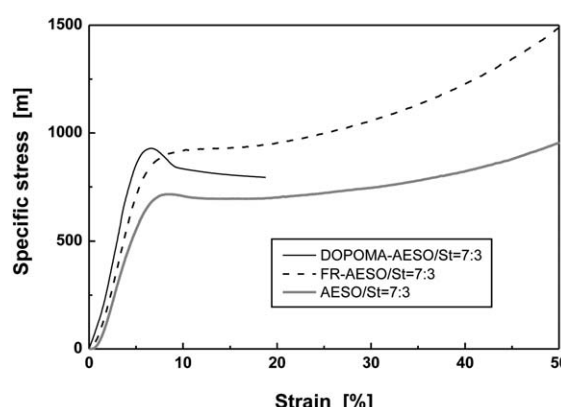


**Fig. 8** Typical compressive specific stress–strain curves of AESO/St, FR-AESO/St and DOPOMA-AESO/St foams (density =  $0.220 \pm 0.005 \text{ g cm}^{-3}$ ).

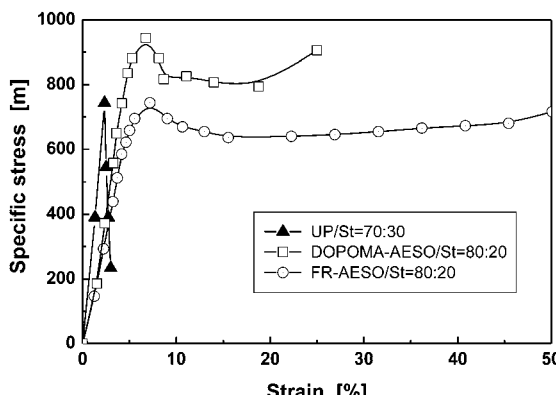


**Fig. 9** Compressive specific stress–strain curves of DOPOMA-AESO/St, FR-AESO/St foams (with 4 phr BPO and 0.4 phr *N,N*-dimethyl aniline) and conventional UP/St foams (with 3 phr BPO and 0.3 phr *N,N*-dimethyl aniline).

the ESO contents in the FR-AESO/St and DOPOMA-AESO/St foams are 45.7 and 54.9 wt%, respectively. The values form a striking contrast to the 38.4 wt% of the aforesaid AESO/St foam. Clearly, another benefit is gained when attaching molecules of the flame retardants to AESO, *i.e.* less monomer derived from fossil resources is sufficient to fabricate the foams with high mechanical strength. Additionally, more natural plant oil in the bio-foams must facilitate biodegradation of the discarded packaging.

Considering that flame retardants have been introduced into the molecules of AESO, flame retardancy of the bio-foams is evaluated in terms of LOI value (Tables 1 and 2). It is demonstrated that a higher LOI value is detected with higher phosphorus content. For FR-AESO/St (70/30) foams, the LOI value increases from 18.5 to 26.5 when the phosphorus content is increased from 0 to 2.54%. Accordingly, the FR-AESO/St foam with the molar ratio of FRC-6-MA/AESO of 3.0 : 1 can be rated as a flame retardant one (note: the basic level of LOI of a flame retardant material is 26). For DOPOMA-AESO/St foams, only 1.93% phosphorus can be attached onto DOPOMA-AESO chains because the reaction system becomes too viscous if more DOPOMA is used. Even so, the DOPOMA-AESO/St foams exhibit a similar LOI value as FR-AESO/St foams in the case of a similar amount of phosphorous.

**Table 1** Flame retardancy of FR-AESO/St foams with different FRC-6-MA contents (FR-AESO/St = 70/30, density =  $0.22 \pm 0.05 \text{ g cm}^{-3}$ )

Molar ratio of FRC-6-MA/AESO	P (%)	N (%)	LOI	UL 94	Char yield (%)
0 : 1	0.00	0.00	18.5	—	3.50
0.5 : 1	0.75	0.34	21.0	—	10.75
1.0 : 1	1.30	0.59	22.5	—	13.75
1.5 : 1	1.72	0.78	23.0	—	17.25
2.0 : 1	2.05	0.93	24.5	V2 <sup>a</sup>	19.50
3.0 : 1	2.54	1.15	26.5	V1 <sup>a</sup>	22.78

<sup>a</sup> V2: burning stops within 30 seconds on a vertical specimen; drips of flaming particles are allowed. V1: burning stops within 30 seconds on a vertical specimen; drips of particles allowed, as long as they are not inflamed.

**Table 2** Flame retardancy of DOPOMA-AESO/St foams with different DOPOMA contents (DOPOMA-AESO/St = 70/30, density =  $0.22 \pm 0.05 \text{ g cm}^{-3}$ )

Molar ratio of DOPOMA/AESO	P (%)	LOI	UL 94	Char yield (%)
0 : 1	0.00	18.5	—	3.50
0.5 : 1	0.79	20.5	—	12.75
1.0 : 1	1.42	22.0	—	15.75
1.5 : 1	1.93	23.5	V2	19.25

The UL 94 vertical test provides another indicator to assess flame retardancy. As shown in Tables 1 and 2, the V1 grade can be achieved for FR-AESO/St foam with 2.54% phosphorus, while DOPOMA-AESO/St foam with 1.93% phosphorus performs as V2 grade. These results agree with the LOI measurements. It is noted that the UL 94 test cannot be carried out for other foams with phosphorus content below 1.72%, implying that phosphorus must be a critical issue in forming chars and arresting the inflammation.

To understand the above antiflaming performance from the point of view of their thermal stability, thermogravimetric analysis of the foams is conducted (Fig. 10). Obviously, AESO/St foam only shows one weight loss peak, while FR-AESO/St and DOPOMA-AESO/St foams give two weight loss steps. The first one between 150 and 220 °C should be attributed to the decomposition of phosphorus groups (Table S1†), which leads

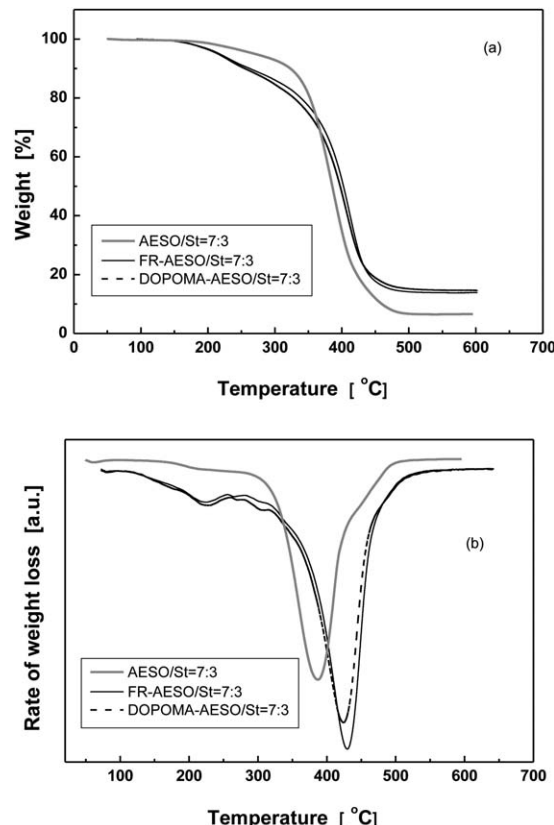


**Fig. 10** (a) TGA and (b) DTG curves of AESO/St, FR-AESO/St and DOPOMA-AESO/St foams measured in  $\text{N}_2$ .

**Table 3** Flame retardancy of IFR-AESO/St (7/3) foams with different IFR contents in comparison to that of FR-AESO/St (7/3) and DOPOMA-AESO/St (7/3) foams (density =  $0.22 \pm 0.05 \text{ g cm}^{-3}$ )

Foams	LOI	UL 94	Char yield (%)
IFR-AESO/St (IFR/AESO = 0/100)	18.5	No self-extinguishing property	3.50
IFR-AESO/St (IFR/AESO = 20/80)	23.5	No self-extinguishing property	12.75
IFR-AESO/St (IFR/AESO = 30/70)	26.0	V1	18.25
IFR-AESO/St (IFR/AESO = 40/60)	28.5	V1	28.40
FR-AESO/St (FRC-6-MA/AESO = 3/1)	26.5	V1	22.78
DOPOMA-AESO/St (DOPOMA/AESO = 1.5/1)	23.5	V2	19.25

to formation of a protection layer on the polymer chains.<sup>32</sup> As a result, the peak temperature of the second step originating from main chain decomposition is raised by about  $40^\circ\text{C}$  and the char yield increases with phosphorus content (Tables 1 and 2). Comparatively, the char yield of DOPOMA-AESO/St foams is higher than that of FR-AESO/St foams owing to the higher aromatic content of DOPO. Increasing the char formation limits the production of combustible gases, decreases the exothermicity of the pyrolysis reaction, reduces thermal conductivity of the burning materials and consequently lowers flammability of the material.

With respect to the extrinsic flame retarding strategy, it is noted that the LOI value, UL 94 grade and char yield of IFR-AESO/St foam increase with the content of the intumescent

flame retardant (Table 3). The comparison between the intumescent systems and intrinsic antiflaming bio-foams shows that the addition of 30 wt% IFR to AESO brings about a comparable LOI value and UL 94 grade as FR-AESO/St (FRC-6-MA/AESO = 3/1). Further increasing IFR content to 40 wt% can continually promote the LOI value of IFR-AESO/St foam, but its UL 94 grade remains unchanged. In fact, incorporation of IFR significantly brings down mechanical properties of IFR-AESO/St foams (Fig. 11), which follows the general rule of particulate filled polymer composites as a result of poor dispersion and weak interfaces. Especially, when IFR content is only 20 wt%, the foam starts to perform like a soft material without yielding. Since at least 30 wt% IFR is needed to obtain acceptable flame retardancy, it is thus known that the foams are not suitable for structural applications. An intrinsic antiflaming method by introducing phosphorus to the molecular chains is more efficient to produce bio-foams with combined prominent mechanical properties and excellent flame retardancy.

### Biodegradation of FR-AESO foams in soil

We have proven that FR-AESO/St foams have inherent inflaming retardancy and exhibit similar compressive stress, but higher ductility in comparison with commercially used UP foam. Therefore, it would be desirable to know whether the bio-foams have inherited the biodegradability of plant oil. Fig. 12 shows that this is the case, and a higher ratio of FR-AESO corresponds

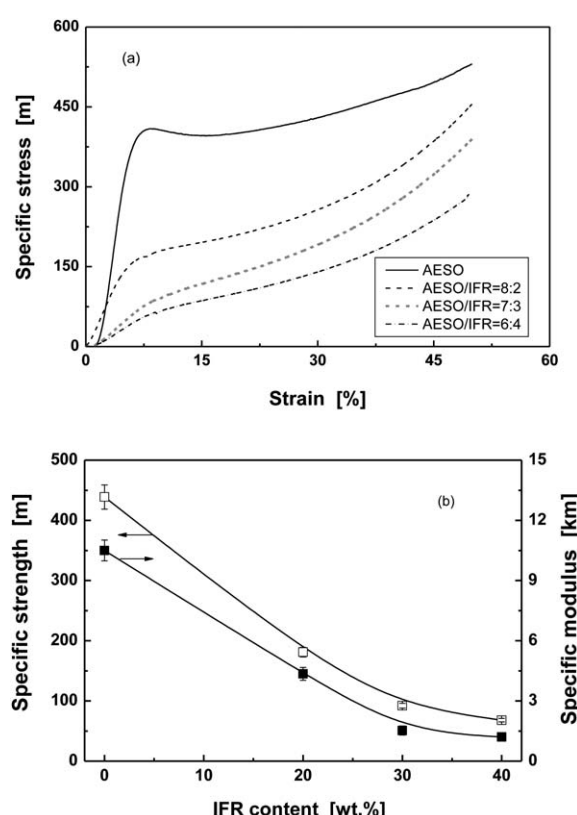


**Fig. 11** (a) Typical compressive specific stress-strain curves and (b) compressive properties of IFR-AESO/St foams with different IFR contents (AESO/St = 7/3, density =  $0.220 \pm 0.005 \text{ g cm}^{-3}$ ).

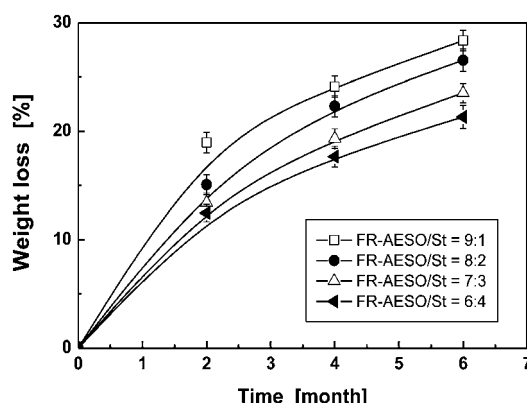


**Fig. 12** Time dependence of soil burial biodegradation induced weight loss of FR-AESO/St foams cured with 4 phr BPO and 0.4 phr *N,N*-dimethyl aniline at various FR-AESO/St ratios (density =  $0.20 \pm 0.01 \text{ g cm}^{-3}$ ).

to a higher weight loss of FR-AESO/St foams at the same soil burial time. It means that the triglyceride molecular structure remained when AESO is converted into FR-AESO, and the chemically introduced flame retardants do not obstruct biodegradability of AESO. In fact, more ester groups are produced when the flame retardant FRC-6 is grafted onto AESO in addition to those brought by FRC-6 itself (Scheme 1). These weak sites would be easily attacked by fungi and improve biodegradation of the foams. The conclusion is supported by the plots in Fig. 13, which shows that FR-AESO/St foams have similar weight loss as AESO/St foams with an identical St content. This means that the main controlling factors of their biodegradation manner are the same, *i.e.* ester groups and double bonds. Ester

groups are favorable to biodegradation of the bio-foams, while double bonds produce a higher crosslink density that restricts biological degradation.

Morphologies of the foams before and after the soil burial test lasting six months are shown in Fig. 14. For the foam with less St (*e.g.*, FR-AESO/St = 80/20), the cellular structures are completely destroyed due to the serious biodegradation. In contrast, the cellular structures can still be identified for the foams with higher St content (*e.g.*, FR-AESO/St = 60/40). These observations coincide with the above-mentioned variation in weight loss. That is, the comonomer St favors the foams with higher compressive properties, but slows down their biodegradation.

## Conclusions

In this work, two kinds of maleic anhydride modified phosphorus-containing flame retardants were grafted onto AESO molecules, forming two functional bio-resins, FR-AESO and DOPO-AESO. Based on these resins, two kinds of flame retardant bio-foams were successfully produced. Owing to the appearance of additional double bonds or biphenyl groups on the AESO chains, the bio-foams have acquired improved mechanical properties in addition to satisfying antiflaming and biodegradable properties, which enable them to be used for structural applications as conventional unsaturated polyester foams. The reactive flame retardants partially took the role of styrene, so that more soybean oil can be introduced into the bio-foams, without lowering their compressive strength. Accordingly, the foams' toughness and biodegradability are also raised. The molecular design and synthesis proposed by the authors are evidently superior to the approach of using additive flame retardant. For example, the FR-AESO/St foams (FRC-6-MA/AESO = 3/1, FR-AESO/St = 70/30) showed an antiflaming capability similar to the AESO foams filled with 30 wt% intumescence flame retardant, but the former possesses much higher mechanical properties than the latter. On the other hand, the FR-AESO/St foams kept the biodegradability of renewable resources, as demonstrated by evident weight loss and damage of cellular structures after soil burial. Integration of intrinsic flame retardancy into AESO molecules proves that it makes no difference to the biodegradability of the resultant foams.

## Acknowledgements

The authors are grateful to the financial support by the Program of Science and Technology, the Education Department of Guangdong (Grant: cxzd1001), the Program of the Science and Technology, Department of Guangdong (Grant: 2007A010500004) and the Sino-Hungarian Scientific and Technological Cooperation Project (CHN-19/2004).

## Notes and references

- 1 A. K. Mohanty, M. Misra and G. Hinrichsen, *Macromol. Mater. Eng.*, 2000, **276/277**, 1.

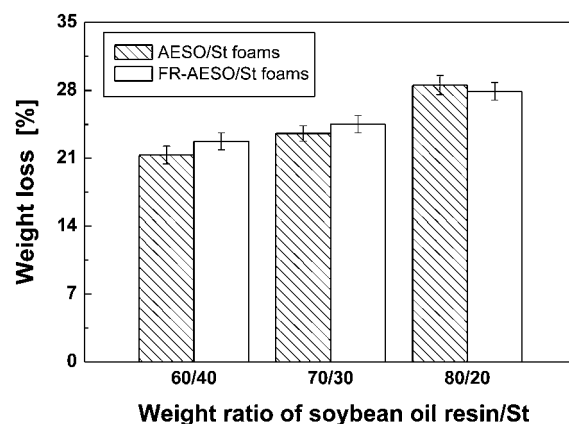


**Fig. 13** Weight loss of AESO/St foams and FR-AESO/St foams after soil burial for 6 months. The foams were cured with 4 phr BPO and 0.4 phr *N,N*-dimethyl aniline (density =  $0.20 \pm 0.01 \text{ g cm}^{-3}$ ).

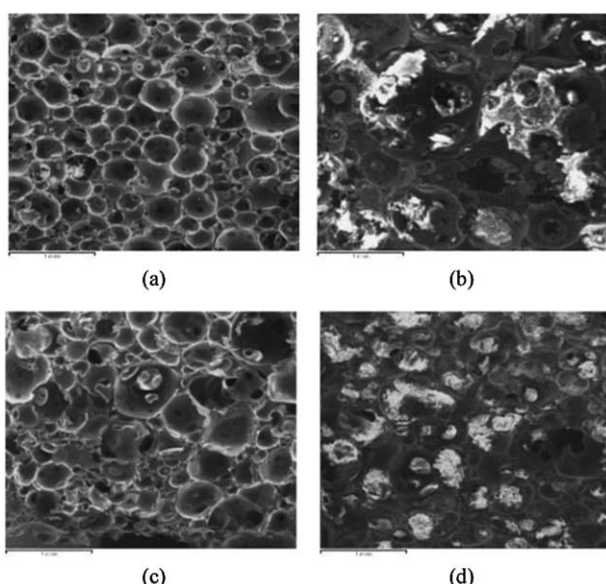


**Fig. 14** Soil burial biodegradation induced variation in morphologies of (a and b) FR-AESO/St (80/20) foam and (c and d) FR-AESO/St (60/40) foam cured with 4 phr BPO and 0.4 phr *N,N*-dimethyl aniline (density =  $0.20 \pm 0.01 \text{ g cm}^{-3}$ ). (a and c) Before soil burial, (b and d) after soil burial for 6 months.



2 W.-Y. Guo, D.-J. Yang, R. Li and X. Q. Qiu, *Acta Polym. Sin.*, 2012, (9), 988.

3 J. Gu, L. Lin, Y.-F. Luo and D.-M. Jia, *Acta Polym. Sin.*, 2012, (8), 852.

4 J. F. Zhang and X. Z. Sun, *J. Appl. Polym. Sci.*, 2007, **106**, 857.

5 S. Blanche and X. Z. Sun, *Adv. Polym. Technol.*, 2004, **23**, 277.

6 Y. Nabar, R. Narayan and M. Schindler, *Polym. Eng. Sci.*, 2006, **46**, 438.

7 J. J. Guan and M. A. Hanna, *Biomacromolecules*, 2004, **5**, 2329.

8 D. Preechawong, M. Peesan, R. Rujiravanit and P. Supaphol, *Macromol. Symp.*, 2004, **216**, 217.

9 J. L. Willett and R. L. Shogren, *Polymer*, 2002, **43**, 5935.

10 J. Y. Cha, D. S. Chung, P. A. Seib and M. A. Hanna, *Ind. Crops Prod.*, 2001, **14**, 23.

11 J. Y. Cha, D. S. Chung and P. A. Seib, *Trans. ASAE*, 1999, **42**, 1765.

12 R. L. Shogren, J. W. Lawton, W. M. Doane and K. F. Tiefenbachers, *Polymer*, 1998, **39**, 6649.

13 R. L. Shogren, *Carbohydr. Polym.*, 1996, **29**, 57.

14 S. Hatnagar and M. A. Hanna, *Trans. ASAE*, 1995, **38**, 567.

15 G. M. Glenn and D. W. Irving, *Cereal Chem.*, 1995, **72**, 155.

16 J. W. Lawton, R. L. Shogren and K. F. Tiefenbacher, *Ind. Crops Prod.*, 2004, **19**, 41.

17 G. M. Ganjyal, N. Reddy, Y. Q. Yang and M. A. Hanna, *J. Appl. Polym. Sci.*, 2004, **93**, 2627.

18 J. Guan and M. A. Hanna, *Ind. Crops Prod.*, 2004, **19**, 255.

19 D. S. Ogunniyi, *Bioresour. Technol.*, 2006, **97**, 1086.

20 D. A. Don, W. F. McSherry and L. A. Goldblatt, *J. Am. Oil Chem. Soc.*, 1959, **36**, 16.

21 G. Mothé and C. R. de Araújo, *Thermochim. Acta*, 2000, **357-358**, 321.

22 A. Guo, I. Javni and Z. Petrovic, *J. Appl. Polym. Sci.*, 2000, **77**, 467.

23 I. Javni, W. Zhang and Z. Petrovic, *J. Polym. Environ.*, 2004, **12**, 123.

24 H. J. Wang, M. Z. Rong, M. Q. Zhang, J. Hu and T. Czigány, *Biomacromolecules*, 2008, **9**, 615.

25 S. P. Wu, M. Z. Rong and M. Q. Zhang, *J. Biobased Mater. Bioenergy*, 2007, **1**, 417.

26 S. P. Wu, J. F. Qiu, M. Z. Rong, M. Q. Zhang and L. Y. Zhang, *Polym. Int.*, 2009, **58**, 403.

27 S. P. Wu, M. Z. Rong, M. Q. Zhang and J. Hu, *Acta Polym. Sin.*, 2007, (10), 993.

28 H. J. Wang, M. Z. Rong, M. Q. Zhang and T. Czigány, *Compos. Interfaces*, 2008, **15**, 95.

29 J. Lu, S. Khot and R. P. Wool, *Polymer*, 2005, **46**, 71.

30 J. Lu and R. P. Wool, *Compos. Sci. Technol.*, 2008, **68**, 1025.

31 Y. L. Liu, *Polymer*, 2001, **42**, 3445.

32 S. V. Levchik and E. D. Weil, *Polym. Int.*, 2004, **53**, 1901.

